

Real-Time Distribution System Topology Monitoring with Limited Communication

Hongyi Wei¹, Yuxiao Liu¹, Qingchun Hou¹, Mingxuan Li¹, Fei Teng², Ning Zhang^{1*}, Chongqing Kang¹

1 Department of Electrical Engineering, Tsinghua University, Beijing 100084, China

2 Control and Power Research Group, Department of Electrical and Electronic Engineering, Imperial College London

ABSTRACT

Real-time topology monitoring brings in high communication investments and operating costs. This paper proposes a real-time topology monitoring method using only voltage magnitude measurements from partial critical buses for real-time communication, which reduces communication requirement and network traffic greatly. A three-step angle-free optimization algorithm framework is designed to estimate current topology. Firstly, we perform load forecasting and power flow calculation to generate enough pseudo measurements, which makes up the lack of real-time measurements. Secondly, weighted least square method and improved extended Kalman filter are used to eliminate static and dynamic noises. These state estimation methods help provide more accurate measurements for topology tracking, especially with plenty of pseudo-measurements and accumulated error caused by load forecasting. Finally, we design an angle-free topology tracking algorithm based on voltage magnitude measurements of critical buses to estimate and correct current topology. Numerical results on IEEE 33-bus case show that our framework with only 10 critical buses reaches a high real-time topology monitoring accuracy $F1$ of 91.59% and thus can greatly reduce communication requirement.

Keywords: Topology tracking, limited real-time measurements, communication costs, angle-free topology tracking algorithm, state estimation

NONMENCLATURE

Abbreviations

AMI	Advanced Metering Infrastructure
EKF	Extended Kalman Filter
MDMS	Meter Data Management System
PMU	Phasor Measurement Unit
WLSM	Weighted Least Square Method

Symbols

$\mathbf{v}_{1,i}$	The i^{th} critical bus
$\mathbf{v}_{2,j}$	The j^{th} non-critical bus
l	Branch number
m	Critical bus number
n	Bus number (except reference bus)
t	Time point
p_i	Active power of the i^{th} bus
q_i	Reactive power of the i^{th} bus
v_i	Voltage magnitude of the i^{th} bus
θ_i	Voltage angle of the i^{th} bus
C	Communication network traffic
T_1	Real-time communication interval
T_2	System communication interval
ϵ_t	System topology in t time point

1. INTRODUCTION

Accurate topology in power distribution networks is the prerequisite of system operation. In actual distribution networks, system topology may frequently change because of unexpected line cut off or power line overload [1], sometimes up to five to ten times a day [2]. Hence, real-time topology monitoring is essential in smart distribution grid.

However, in most distribution networks, the terminal measurements are not accurate and real-time

communication capacity is insufficient. The solution is to deploy advanced metering infrastructure (AMI) improving full-scale measurement precision and the communication capacity, which is shown in Fig. 1.

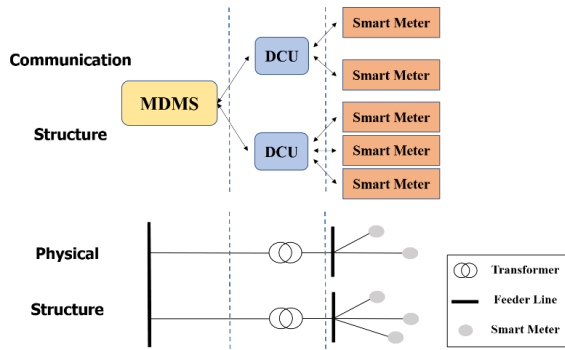


Fig 1 AMI structure in distribution systems

Although AMI can collect data at terminal buses and transmit them to meter data management system (MDMS) instantly, the communication costs are extremely high because of its high capacity. In 2015, communication related costs make up nearly 50% of all American AMI investments when pilot deployed [3]. The whole communication costs are composed of equipment investments and operating costs. As wireless communication gradually replaces traditional power line communication in distribution systems, system operators sometimes invest private networks to instantly transmit important measurements, which causes large equipment investments. However, if operators rent public networks, they must pay for their huge network traffic. In Illinois' projects, these two costs make up 15.5% and 58% of whole equipment investments and operating costs separately [4]. Thus, it is in needs of reducing real-time communication capacity to cut the costs.

Some researches aim at identifying system topology based on limited measurements to save both communication deployment costs and measurement devices costs. Bariyac chooses a few buses to install phasor measurement unit (PMU) and utilizes time series voltages to monitor system topology [5]. However, it utilizes a few PMU, which incurs high costs. Besides, as this method must receive series voltage measurements (typically in the order of seconds), it also increases network traffic. Cavraro proposes a meter placement strategy based on smart meter measurements to recovery partial topology [6]. This work assumes only several branches can switch and places meters around them. Apparently, it cannot monitor other branches' states once they switch. Therefore, if using this method,

there would be more communication deployment costs to monitor whole system topology accurately.

Different from the above studies, we address the problem of saving both communication deployment costs and operating costs when monitoring whole topology with a higher accuracy. We propose a framework that utilizes "critical" buses instead of all buses to transmit real-time measurements and then monitors current topology in MDMS, while other "non-critical" buses keep a longer communication interval. [7] has stated the feasibility using sparse smart meters to observe distribution system As MDMS is able to communicate with smart meters bi-directionally to control each meter's communication interval, we can select whether one meter is critical [8]. The contribution of our work is summarized as follows:

- 1) We address the problem of real-time distribution system topology monitoring with limited communications. Our approach can largely save the communication costs and still maintain a high topology monitoring frequency.
- 2) We propose a bi-level optimization algorithm framework using limited communication. The upper optimization algorithm estimates current topology with the least loss iteratively. The lower one generates pseudo measurements and performs state estimation to improve topology estimation accuracy.

2. REAL-TIME TOPOLOGY MONITORING FRAMEWORK

The framework shown in Fig. 2 is designed in the requirement of accurately estimating system states with limited noisy measurements. Since line parameters remain unchanged during a long time, we assume they are already known or identified by algorithms like [9]-[11]. Further, the topology ϵ_{t-1} of previous states in time point $t - 1$ is also known. We firstly perform load forecasting to generate enough pseudo measurements. Then state estimation methods are implemented to reduce measurement noises, which includes weighted least square method (WLSM) and improved extended Kalman filter (EKF). After that, we check whether topology has changed during T_1 by calculating voltage loss. If changed, we perform the above processes to estimate the optimal topology $\hat{\epsilon}_t$ iteratively.

2.1 Generating pseudo measurements

We utilize day-ahead load forecasting method to generate pseudo measurements of forecasted active power \bar{P}_t and reactive power \bar{Q}_t , which are given by linear regression models:

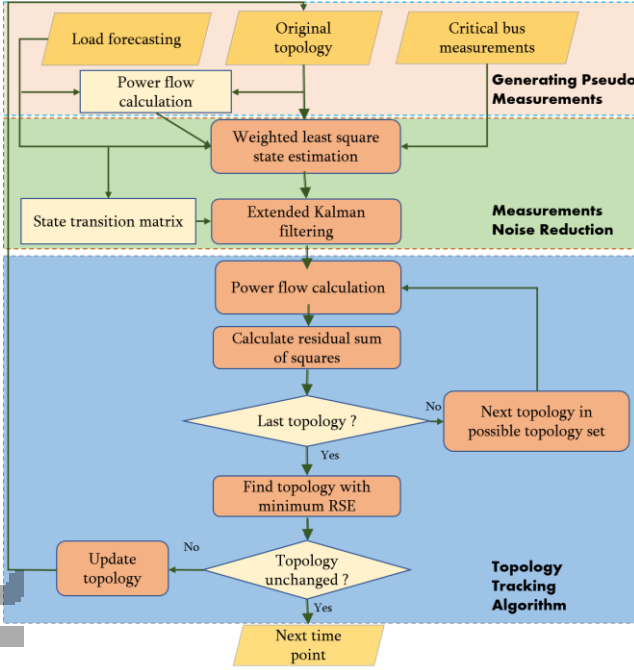


Fig 2 Real-time topology monitoring framework

$$\tilde{p}_{i,t} = a_{i,t-1}p_{i,t-1} + b_{i,t-1}, \quad (1a)$$

$$\tilde{q}_{i,t} = c_{i,t-1}q_{i,t-1} + d_{i,t-1}, \quad (1b)$$

where $\tilde{p}_{i,t}$ and $\tilde{q}_{i,t}$ are the elements of $\tilde{\mathbf{P}}_t$ and $\tilde{\mathbf{Q}}_t$ separately in i^{th} bus at time point t . While $a_{i,t-1}$, $b_{i,t-1}$, $c_{i,t-1}$ and $d_{i,t-1}$ are elements of \mathbf{A}_{t-1} , \mathbf{B}_{t-1} , \mathbf{C}_{t-1} and \mathbf{D}_{t-1} .

Then, we utilize the decoupled linearized power flow method in [12] to calculate the pseudo measurements of voltage magnitude \tilde{V}_t and angle $\tilde{\theta}_t$:

$$\begin{bmatrix} \tilde{V}_t \\ \tilde{\theta}_t \end{bmatrix} = \mathbf{Y}_1 \begin{bmatrix} \tilde{\mathbf{P}}_t \\ \tilde{\mathbf{Q}}_t \\ \mathbf{1} \end{bmatrix}, \quad (2)$$

where \mathbf{Y}_1 is linearized power flow coefficient matrix calculated based on current topology with $2n$ rows and $2n + 1$ columns.

2.2 Measurement noise reduction

When critical buses transmit their real-time measurements to MDMS, all measurements must be filtered to reduce noises. We use WLSM to estimate voltage magnitudes \hat{v} and angle $\hat{\theta}$. However, the rolling forecasting brings accumulated error in pseudo measurements, which disturbs WLSM. Therefore, we use improved EKF to track the dynamic error. We perform WLSM method when real-time communication happens while improved EKF method is iterated during a system communication interval to get the estimated results $\hat{\mathbf{x}}_t$.

There are many state estimation methods used in distribution system, where WLSM is one of the most

widely used methods [13]. The measurement equation model is:

$$\mathbf{z} = \mathbf{h}(\mathbf{x}) + \mathbf{v}, \quad (3)$$

where \mathbf{z} denotes all measurements, including \mathbf{v} , \mathbf{p} , \mathbf{q} , θ . $\mathbf{h}(\mathbf{x})$ is the measurement function and \mathbf{v} is the measurement noise. The goal of WLSM is to minimize the weighted residual sum of squares of \mathbf{v} :

$$\min_{\mathbf{x}} J(\mathbf{x}) = \frac{1}{2} [\mathbf{z} - \mathbf{h}(\mathbf{x})]^T \mathbf{W} [\mathbf{z} - \mathbf{h}(\mathbf{x})], \quad (4)$$

where \mathbf{x} denotes the state variables including voltage magnitudes and angles. \mathbf{W} represents the weighted matrix which is the inverse of measurement noise covariance. We use Newton method to get the solution and denote the Jacobian matrix of $\mathbf{h}(\mathbf{x})$ as $\mathbf{H}(\mathbf{x})$. Therefore, we can iteratively solve the problem:

$$\mathbf{x}_{k+1} = \mathbf{x}_k + \mathbf{G}_k^{-1} \mathbf{H}(\mathbf{x}_k)^T \mathbf{W} [\mathbf{z} - \mathbf{h}(\mathbf{x}_k)], \quad (5)$$

where \mathbf{G}_k is the gain matrix in the k^{th} iteration:

$$\mathbf{G}_k = \mathbf{H}(\mathbf{x}_k)^T \mathbf{W} \mathbf{H}(\mathbf{x}_k). \quad (6)$$

After several iterations, we can get the estimated state variables $\hat{\mathbf{x}}_t$.

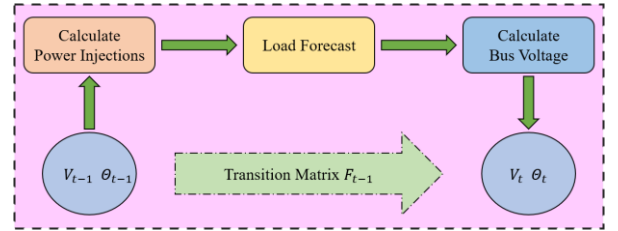


Fig 3 Transition matrix linearization process

However, WLSM cannot maintain a good performance dealing with accumulated error, especially after a long time period of rolling forecasting. So, we introduce improved EKF method. As Kalman filter methods are designed for linear time-invariant system, we need to linearize the transition matrix. Here we analyze the transition matrix based on load forecast to get a more explainable result, which is shown in Fig. 3. Besides, both transition noise and measurement noise must have a Gaussian distribution with a mean $\mu = 0$ and variance σ^2 [14]. The covariance matrices of transition noise and measurement noise are denoted as \mathbf{R} and \mathbf{Q} separately. However, the actual transition noise is non-Gaussian and should be approximated to Gaussian. Traditional EKF method firstly utilizes transition matrix to get updated state variables from time point $t - 1$ to t :

$$\tilde{\mathbf{x}}_{t|t-1} = \mathbf{F}_{t-1} \tilde{\mathbf{x}}_{t-1|t-1}, \quad (7)$$

where $\tilde{\mathbf{x}}_{t|t-1}$ represents the forecasted state variables at t . To get the linearized \mathbf{F}_{t-1} matrix from load forecasting, we need to calculate $\tilde{\mathbf{P}}_{t-1}$ and $\tilde{\mathbf{Q}}_{t-1}$ from $\tilde{\mathbf{V}}_{t-1}$ and $\tilde{\theta}_{t-1}$, so we linearize the power flow as:

$$\begin{bmatrix} \tilde{\mathbf{P}}_{t-1} \\ \tilde{\mathbf{Q}}_{t-1} \end{bmatrix} = \mathbf{Y}_2 \begin{bmatrix} \tilde{\mathbf{V}}_{t-1} \\ \tilde{\mathbf{\Theta}}_{t-1} \end{bmatrix}, \quad (8)$$

where \mathbf{Y}_2 is the linearized admittance matrix with $2n$ rows and $2n + 2$ columns (including the reference bus). Then we utilize equation (1) and equation (2) to get $\tilde{\mathbf{V}}_t$ and $\tilde{\mathbf{\Theta}}_t$. As \mathbf{Y}_1 and \mathbf{Y}_2 have different dimensions, we need to divide \mathbf{Y}_1 into two submatrices \mathbf{Y}_{11} and \mathbf{Y}_{12} in juxtaposition, which are the first $2n$ columns and the last columns in \mathbf{Y}_1 separately:

$$\mathbf{Y}_1 = \begin{bmatrix} \mathbf{Y}_{11} & \mathbf{Y}_{12} \end{bmatrix}. \quad (9)$$

Therefore, the linearized transition matrix is:

$$\mathbf{F}_t = \mathbf{Y}_{11} \begin{bmatrix} \mathbf{A}_{t-1} & \mathbf{0} \\ \mathbf{0} & \mathbf{C}_{t-1} \end{bmatrix} \mathbf{Y}_2. \quad (10)$$

So, the transition equation (7) can be written as:

$$\tilde{\mathbf{x}}_{t|t-1} = \mathbf{F}_{t-1} \tilde{\mathbf{x}}_{t-1|t-1} + \left(\mathbf{Y}_{11} \begin{bmatrix} \mathbf{B}_{t-1} \\ \mathbf{D}_{t-1} \end{bmatrix} + \mathbf{Y}_{12} \right). \quad (11)$$

After that, we forecast the transition noise covariance matrix in $t + 1$ by:

$$\mathbf{P}_{t|t-1} = \mathbf{F}_{t-1} \mathbf{P}_{t-1|t-1} \mathbf{F}_{t-1}^T + \mathbf{R}_t. \quad (12)$$

Equation (12) updates the covariance matrix utilizing transition matrix. Then, we need to calculate Kalman gain \mathbf{K}_t :

$$\mathbf{K}_t = \mathbf{P}_{t|t-1} \mathbf{H}(\mathbf{x}_{t-1})^T [\mathbf{Q}_t + \mathbf{H}(\mathbf{x}_{t-1}) \mathbf{P}_{t|t-1} \mathbf{H}(\mathbf{x}_{t-1})^T]^{-1}. \quad (13)$$

Equation (13) shows that Kalman gain \mathbf{K}_t is related to $\mathbf{P}_{t|t-1}$ and larger $\mathbf{P}_{t|t-1}$ means \mathbf{K}_t focuses more on feedback. Finally, we correct state variables and get the estimated results dynamically:

$$\tilde{\mathbf{x}}_{t|t} = \tilde{\mathbf{x}}_{t|t-1} + \mathbf{K}_t [\mathbf{z}_t - \mathbf{h}(\tilde{\mathbf{x}}_{t|t-1})], \quad (14)$$

$$\mathbf{P}_{t|t} = [\mathbf{I} - \mathbf{K}_t \mathbf{H}(\mathbf{x}_{t-1})] \mathbf{P}_{t|t-1}. \quad (15)$$

Equation (15) reduces noises from state variables and corrects \mathbf{P} in t .

We then formulate the improved EKF method with two steps: substitute forecasted state variables with WLSM results and introduce transition noise mean as input variables. The substitution relies on the fact that WLSM filters noises from forecasted results. To cope with non-Gaussian noise distribution, we use an approximate Gaussian distribution of transition noise with a mean $\boldsymbol{\mu}$, which is correlated with time. Hence, we can take the noise mean $\boldsymbol{\mu}_t$ as an input variable and rewrite equation (7) as:

$$\tilde{\mathbf{x}}_{t|t-1} = \hat{\mathbf{x}}_t + \boldsymbol{\mu}_t, \quad (16)$$

2.3 Topology tracking algorithm

In this section, we choose the topology that best fits the voltage measurements. To compare the critical bus real-time measurements \mathbf{V}_1 with the estimated values, we use non-critical bus voltage magnitudes $\hat{\mathbf{V}}_2$ and angles $\hat{\mathbf{\Theta}}_2$ with critical bus load measurements $\mathbf{P}_1, \mathbf{Q}_1$ to calculate the estimated critical bus voltage magnitudes $\hat{\mathbf{V}}_1$. In details, we use the following function

to evaluate how well the topology fits the measurements:

$$J(\epsilon_k) = \sum_{i=1}^m (v_{1,i}^k - \hat{v}_{1,i}^k)^2, \quad (17)$$

where ϵ_k represents the k^{th} topology in the possible topology set \mathcal{E} and $\hat{v}_{1,i}^k$ represents the estimated voltage magnitude in the $\mathbf{V}_{1,i}$ bus using topology ϵ_k . We assume that during real-time communication interval, only one branch is switched on or off. Thus, the topology set includes current topology ϵ_0 and other l topologies with each branch's state switched. The goal is to find the most suitable topology $\hat{\epsilon}_t$ and the algorithm is shown below:

Algorithm 1 Topology tracking algorithm

Input: $\mathcal{E}_t, \hat{\mathbf{V}}_{t,2}, \hat{\mathbf{\Theta}}_{t,2}, \mathbf{P}_{t,1}, \mathbf{Q}_{t,1}, \mathbf{V}_{t,1}$;

Output: $\hat{\epsilon}_t$;

- 1: Initialize $i = 0$;
 - 2: **for** i **do**
 - 3: $\epsilon_t = \epsilon_{t,i}$ and calculate $\hat{\mathbf{V}}_1$ in ϵ_t ;
 - 4: Calculate and store $J(\epsilon_t)$;
 - 5: **end for**
 - 6: Find the minimum $J(\epsilon_k)$ in J ;
 - 7: **if** $k = 0$ **then**
 - 8: $\hat{\epsilon}_t = \epsilon_{t,0}$;
 - 9: **else**
 - 10: $\bar{\epsilon}_t = \epsilon_{t,k}$ and form new topology set $\bar{\mathcal{E}}_t$;
 - 11: Perform subsection 2.1 and 2.2 in $\bar{\mathcal{E}}_{t,0}$;
 - 12: Repeat 1-7 and get \bar{J} ;
 - 13: **if** $\bar{J}(\bar{\epsilon}_{t,0}) < J(\epsilon_{t,0})$ **then**
 - 14: $\hat{\epsilon}_t = \bar{\epsilon}_{t,0}$;
 - 15: **else**
 - 16: $\hat{\epsilon}_t = \epsilon_{t,0}$;
 - 17: **end if**
 - 18: **end if**
-

From algorithm 1, at time point t , we first calculate the loss J of the topology set \mathcal{E}_t . If the topology of the minimum loss $J(\epsilon_t)$ is the original topology $\epsilon_{t,0}$, the estimated topology $\hat{\epsilon}_t$ is ϵ_0 , which means topology does not change. Otherwise, we assume topology has changed to $\epsilon_{t,k}$. Then, repeat subsection 2.1 and 2.2 with the new topology. Calculate the new loss \bar{J} and compare $\bar{J}(\bar{\epsilon}_{t,0})$ with $J(\epsilon_{t,0})$ and choose the topology of the smaller one as $\hat{\epsilon}_t$.

3. CASE STUDY INTRODUCTION

3.1 Data Preparation

The Commission for Energy Regulation in Ireland are used to generate our load data [15]. We select meters with 536 days' data from the first 1000 meters and divide these meters into 32 groups. In each group, we sum the meter readings and perform cubic interpolation to get load with a T_1 of 15 minutes. And 0.1% Gaussian white noises are added to it. We divide the whole data into a training set with 486 days, a validation set with 25 days and a test set with 25 days. We perform load forecasting on the training set and get parameters of improved EKF using both training and validation set.

3.2 Simulation Results

We perform the test on IEEE 33-bus case in MATPOWER 7.0 [16]. We test the performance of our algorithm under different experiment settings, i.e. system communication interval T_2 and critical bus numbers m as they determine communication costs. T_2 is chosen as 1 hour or 4 hours and m is chosen as {5, 10, 16} separately. We select critical bus set O_i corresponding to different m as {11, 13, 16, 18, 32}, {11, 13, 14, 15, 16, 17, 18, 31, 32, 33} and {8, 9, 10, 11, 12, 13, 14, 15, 16, 17, 18, 29, 30, 31, 32, 33}. We randomly choose 10 days from test set and arrange 5 topology switching events one day. The test results are recorded in a confusion matrix. We take the result when $m = 10$, $T_2 = 1h$ and O_2 as an example. There are 49 correct switching detections, 1 wrong switching detections and 8 false switching detections in total. Thus, the confusion matrix is shown in Table 1:

TABLE 1
THE CONFUSION MATRIX

Switching Test	Test Results	
	True	False
Actual Results	True	49
	False	8
		902

The evaluation metrics used are precision P , recall R and $F1$ score. They are defined as:

$$P = \frac{TP}{TP + FP}, R = \frac{TP}{TP + FN}, F1 = \frac{2 \times P \times R}{P + R}. \quad (18)$$

Therefore, we can calculate P , R and $F1$ score corresponding to this test:

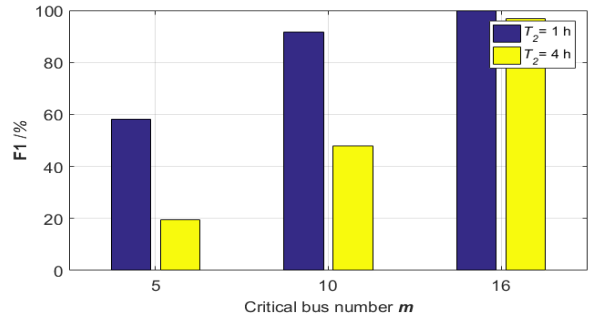
$$P = 85.96\%, R = 98.00\%, F1 = 91.59\%.$$

In this scenario, the network traffic C_1 is much less than original C_0 in real-time communication:

$$C_1 = \frac{m}{n} C_0 = \frac{5}{16} C_0, \quad (19)$$

which is approximately reduced by two third.

Then we analyze other results, $F1$ result is shown in Fig 4. From this result, we find that our framework has a



good performance with limited communication. When m is one third of whole bus number, our framework has a good performance of $F1 = 91.59\%$ with $T_2 = 1h$. Besides, if there are abundant real-time measurements such as m equals half of the whole bus number, our framework still accurately monitors system topology when $T_2 = 4h$ with $F1 = 97\%$. This shows that we can greatly reduce communication capacity by increasing system communication interval using our framework.

Another finding is that shortening T_2 to improve accuracy is valid only when the critical buses are not too few. However, when there are only 5 critical buses chosen from 32, the $F1$ score declines greatly than that when there are more critical buses. Even if we shorten T_2 from 4h to 1h, $F1$ score just increases from 19.4% to 58.1%. It can be concluded that pseudo measurements cannot fully substitute real-time measurements to observe system states.

From Fig 5 and Fig 6, we find that R is higher than 90% at $T_2 = 1h$ and higher than 60% in all tests, which means our framework well tracks true changes.

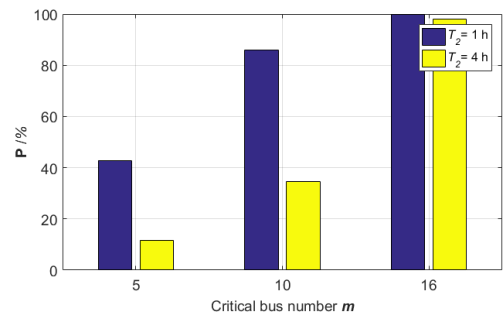


Fig 5 P comparison results with different T_2 and m

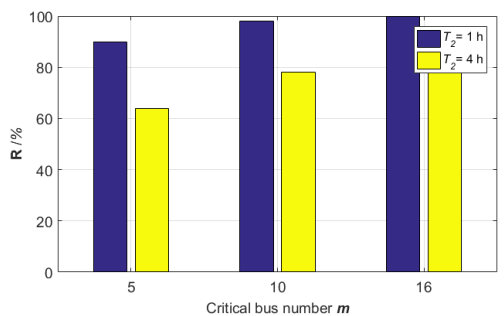


Fig 6 R comparison results with different T_2 and m

However, our framework seems too sensitive to noises because P declines greatly as the number of critical buses decreases. We examine topology detection results when $m=5$ and find that false detection happens continuously during some time (e.g., 2 hours) and often detects the same branch switching wrongly.

4. CONCLUSIONS

Our research addresses the importance of reducing communication capacity in power distribution networks to cut off communication costs. We propose a real-time topology monitoring framework with limited communication. To increase measurements redundancy, the framework utilizes historical data to perform load forecasting, which generates lots of pseudo measurements. Then, most noises of pseudo and real-time measurements are filtered out by WLSM and improved EKF. Finally, a topology tracking algorithm based on critical bus voltage measurements determines the most feasible topology at this time point. We test our framework on IEEE 33-bus case and figure out two conclusions based on the results: 1) The framework monitors system topology with a high accuracy and thus greatly reduces system communication costs. Only one third whole buses chosen as critical buses can accurately track the true topology switching with few false detections. 2) The pseudo measurements cannot fully substitute real-time measurements, which leads to more false detections with few critical buses. In this scenario, shortening system communication interval cannot make up the lack of observation.

Future works will focus on exploring the theoretical lower bound of critical buses with different system communication interval. We will try to balance the network traffic and communication capacity by adjusting system communication interval and critical buses number to reduce more communication costs.

ACKNOWLEDGEMENT

This work was supported by International (Regional) Joint Research Project of National Natural Science Foundation of China (No. 52061635101, 71961137004) and Tsinghua University Initiative Scientific Research Program (20193080026).

REFERENCE

[1] S. J. Pappu, N. Bhatt, R. Pasumarthy, and A. Rajeswaran, "Identifying topology of low voltage distribution networks based on smart meter data," *IEEE Transactions on Smart Grid*, vol. 9, no. 5, pp. 5113–5122, 2017.

[2] A. von Meier, M. L. Brown, R. Arghandeh, L. Mehrmanesh, L. Cibulka, and B. Russ, "Distribution system field study with California utilities to assess

capacity for renewables and electric vehicles," California Energy Commission, Tech. Rep., 2015.

[3] "Advanced metering infrastructure and customer systems," U.S. Department of Energy, Tech. Rep., 2016.

[4] "Advanced metering infrastructure (AMI) cost/benefit analysis," Ameren Illinois, Tech. Rep., 2012.

[5] M. Bariya, A. von Meier, A. Ostfeld, and E. Ratnam, "Data-driven topology estimation with limited sensors in radial distribution feeders," in 2018 IEEE Green Technologies Conference. IEEE, 2018, pp. 183–188.

[6] G. Cavarero, A. Bernstein, V. Kekatos, and Y. Zhang, "Real-time identifiability of power distribution network topologies with limited monitoring," *IEEE Control Systems Letters*, vol. 4, no. 2, pp. 325–330, 2019.

[7] S. Bhela, V. Kekatos, and S. Veeramachaneni, "Enhancing observability in distribution grids using smart meter data," *IEEE Transactions on Smart Grid*, vol. 9, no. 6, pp. 5953–5961, 2017.

[8] N. Uribe-Perez, L. Hernandez, D. De la Vega, and I. Angulo, "State of the art and trends review of smart metering in electricity grids," *Applied Sciences*, vol. 6, no. 3, p. 68, 2016.

[9] J. Yu, Y. Weng, and R. Rajagopal, "Patopaem: A data-driven parameter and topology joint estimation framework for time-varying system in distribution grids," *IEEE Transactions on Power Systems*, vol. 34, no. 3, pp. 1682–1692, 2018.

[10] Zhang, Y. Wang, Y. Weng, and N. Zhang, "Topology identification and line parameter estimation for non-pmu distribution network: A numerical method," *IEEE Transactions on Smart Grid*, 2020.

[11] V. C. Cunha, W. Freitas, F. C. Trindade, and S. Santoso, "Automated determination of topology and line parameters in low voltage systems using smart meters measurements," *IEEE Transactions on Smart Grid*, 2020.

[12] J. Yang, N. Zhang, C. Kang, and Q. Xia, "A state-independent linear power flow model with accurate estimation of voltage magnitude," *IEEE Transactions on Power Systems*, vol. 32, no. 5, pp. 3607–3617, 2016.

[13] Primadianto and C.-N. Lu, "A review on distribution system state estimation," *IEEE Transactions on Power Systems*, vol. 32, no. 5, pp. 3875–3883, 2016.

[14] J. Zhao, M. Netto, and L. Mili, "A robust iterated extended Kalman filter for power system dynamic state estimation," *IEEE Transactions on Power Systems*, vol. 32, no. 4, pp. 3205–3216, 2016.

[15] CER Smart Metering Project—Electricity Customer Behaviour Trial, 2009–2010, Commission for Energy Regulation, Dublin, Ireland, 2012.

[16] R. D. Zimmerman, C. E. Murillo-Sanchez, and R. J. Thomas, "Mat-power: Steady-state operations, planning, and analysis tools for power systems research and education," *IEEE Transactions on power systems*, vol. 26, no. 1, pp. 12–19, 2010.